

Supplementary Information

Indium-Doping-Induced Selenium Vacancy Engineering of Layered Tin Diselenide for Improving Room-Temperature Sulfur Dioxide Gas Sensing

Xuezheng Guo^{a,b,c}, Yijie Shi^b, Yanqiao Ding^b, Yuhui He^d, Bingsheng Du^{a,b,c}, Chengyao Liang^{a,b,c}, Yiling Tan^a, Peilin Liu^a, Xiangshui Miao^d, Yong He^{b,c,*} and Xi Yang^{a,*}

a. Institute of Chemical Materials, China Academy of Engineering Physics, Mianyang 621900, China

b. Key Laboratory of Optoelectronic Technology and Systems of the Education Ministry of China, College of Optoelectronic Engineering, Chongqing University, Chongqing 400044, China

c. State Key Laboratory of Coal Mine Disaster Dynamic and Control, Chongqing University, Chongqing 400044, China

d. School of Integrated Circuits, Huazhong University of Science and Technology, Wuhan 430074, China

X.Z. Guo and Y.J. Shi contributed equally to this work.

**Corresponding authors:*

Yong He

E-mail address: yonghe@cqu.edu.cn

Xi Yang

E-mail address: xyang@caep.cn

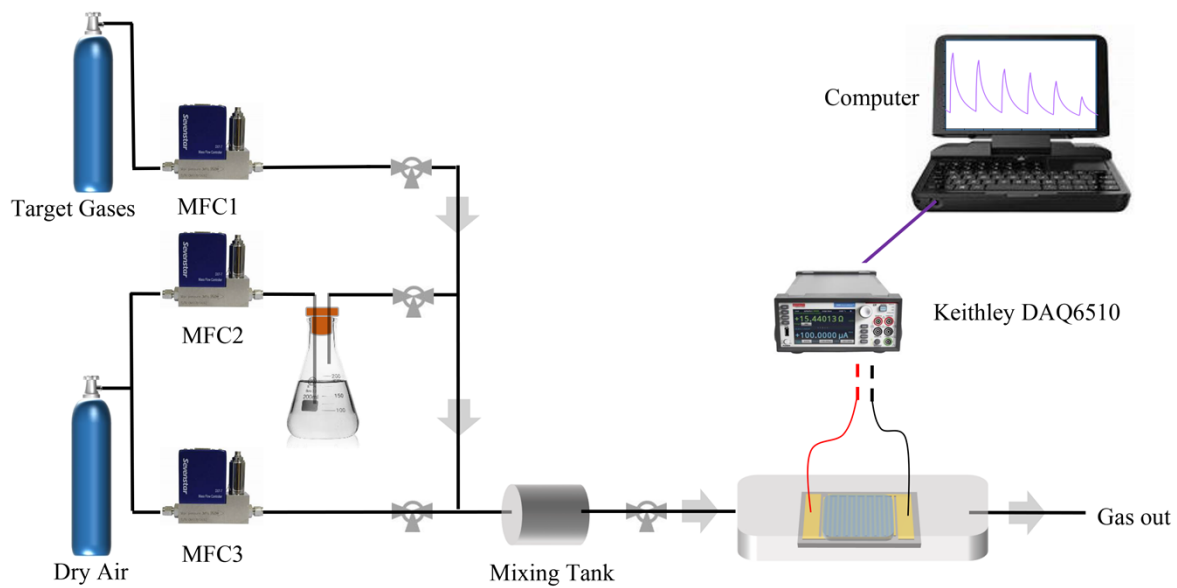


Figure S1. Schematic diagram of gas-sensing procedure.

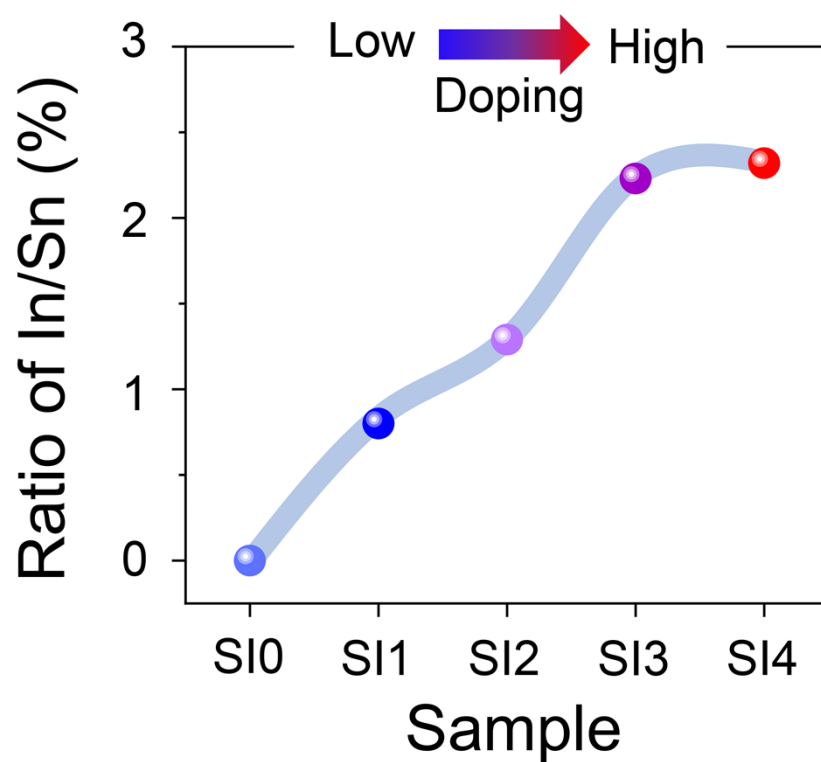


Figure S2. The relationship between In/Sn and the doping samples from ICP-MS.

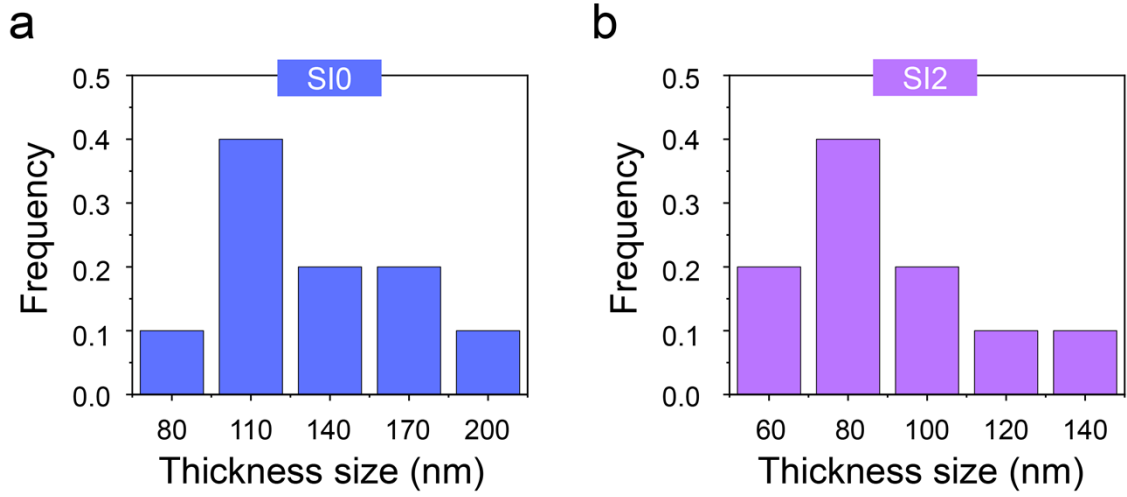


Figure S3. The thickness distribution statistics of (a) S10 and (b) S12 samples.

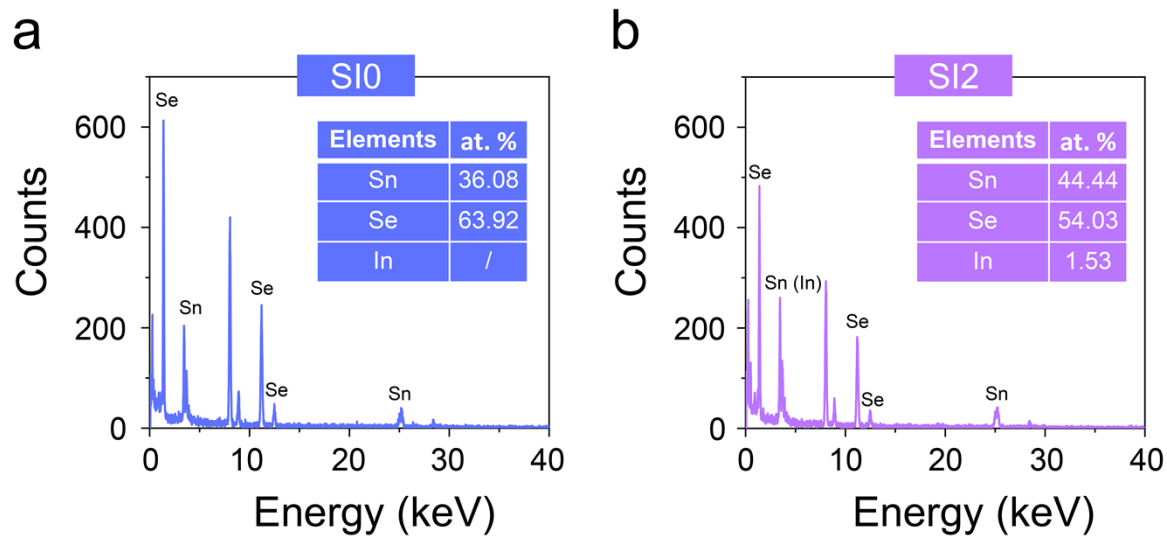


Figure S4. EDS elemental estimations for the (a) S10 and (b) S12 samples.

Table S1. The results of the ratio of the integrated area under each peak in XPS.

XPS – Se 3d	SI0	SI2
Se 3d _{5/2}	38115.54	28031.93
Se 3d _{3/2}	30140.31	26793.88
Se vacancies	2397.61	5027.21

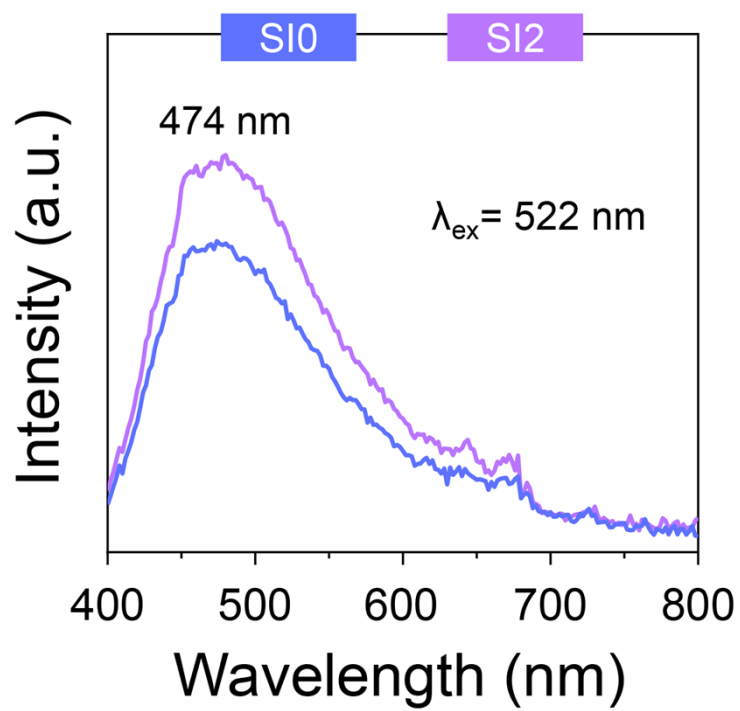


Figure S5. PL spectra of the S10 and S12 samples.

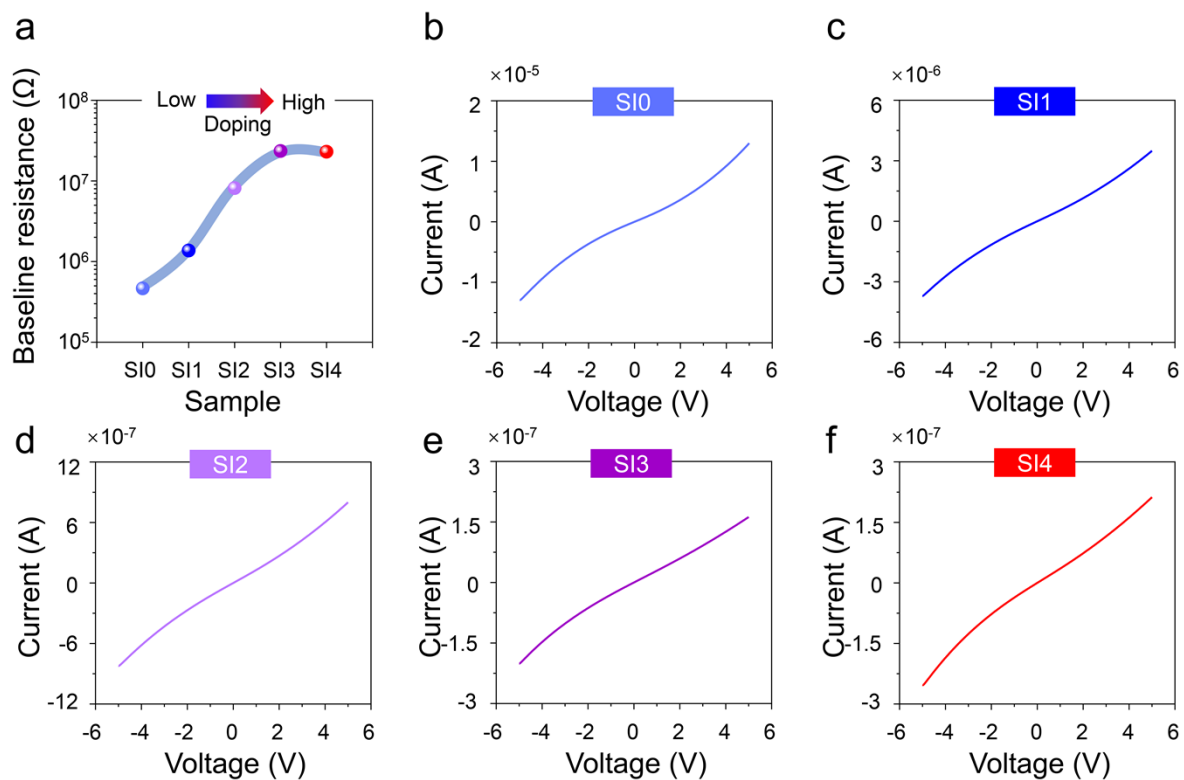


Figure S6. (a) The relationship between baseline resistance and the doping samples. The I-V curves of the (b) SI0, (c) SI1, (d) SI2, (e) SI3, and (f) SI4 samples.

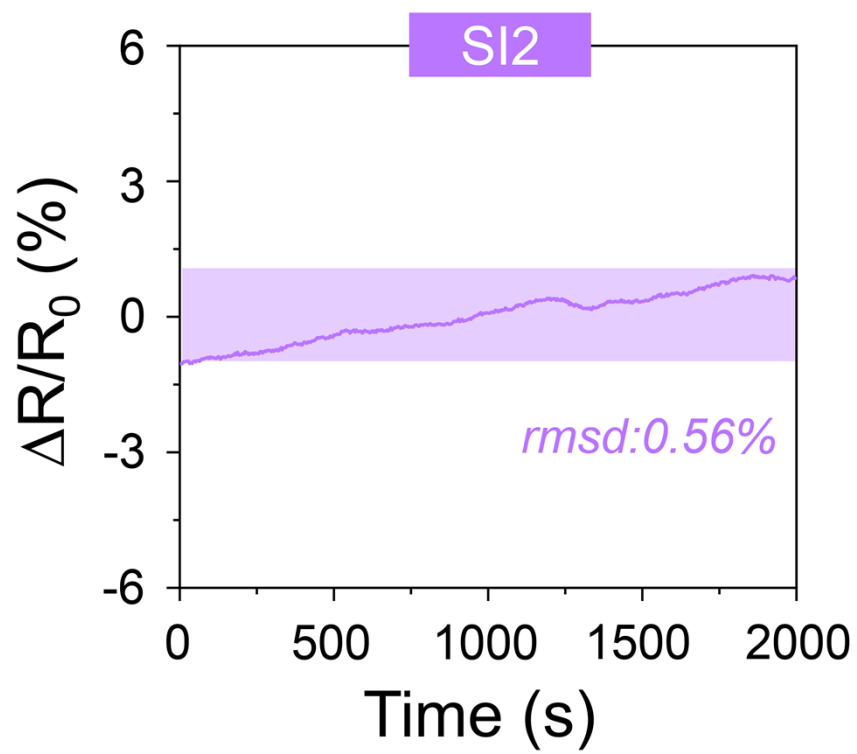


Figure S7. The root-mean-squared deviation noise (rmsd) of the SI2 sensor.

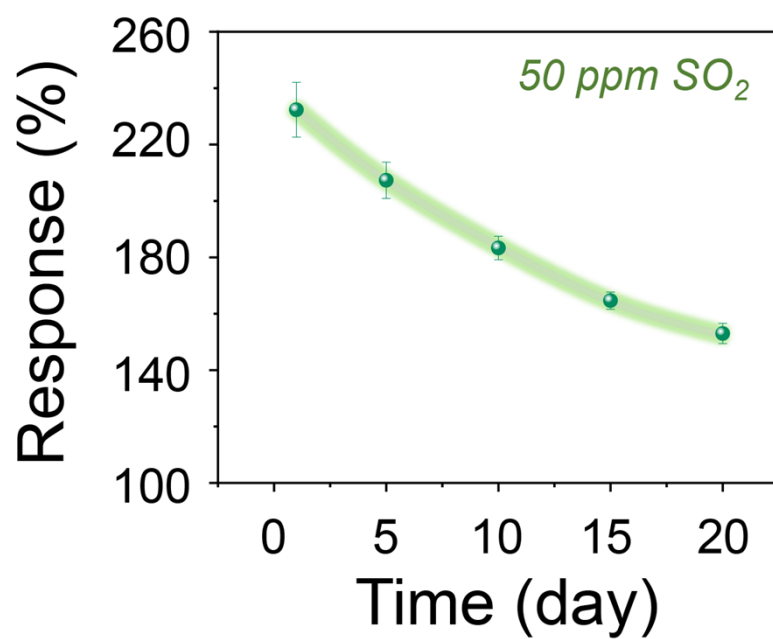


Figure S8. The stability of the SI2 sensor to 50 ppm SO₂.

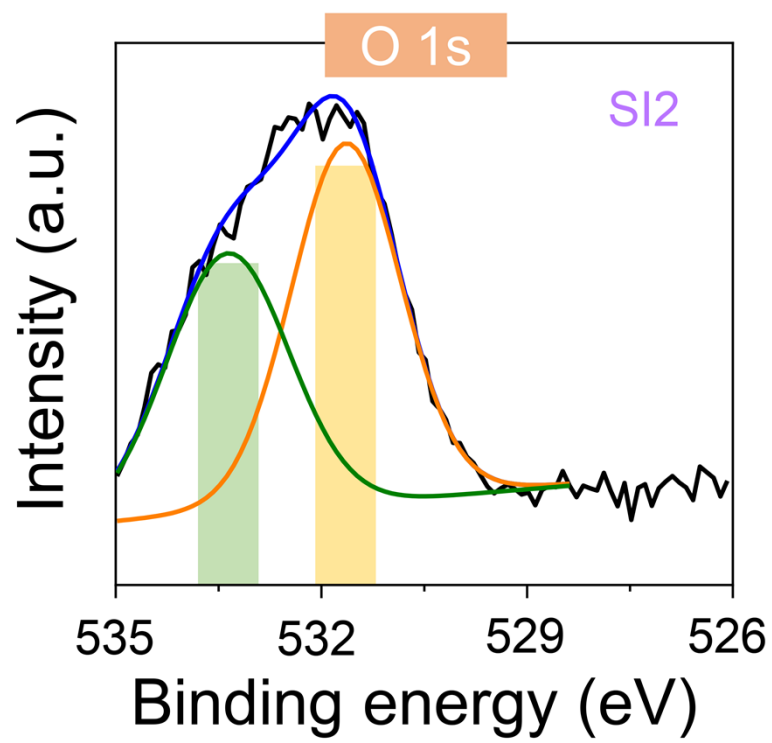


Figure S9. O 1s spectrum of the SI2 sample.

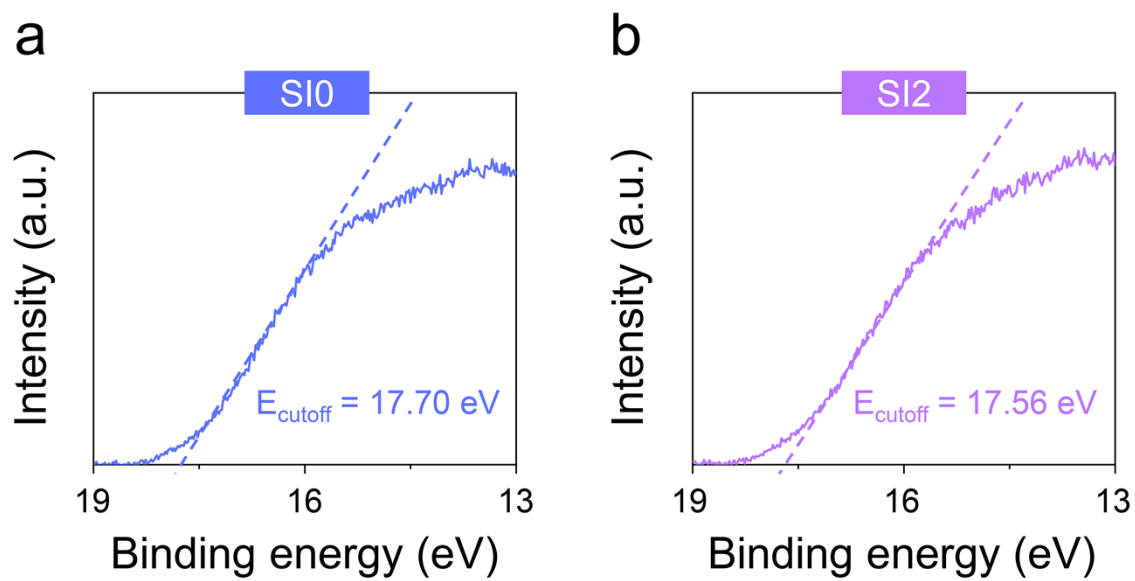


Figure S10. UPS results and the corresponding work functions of (a) SI0 and (b) SI2 samples.

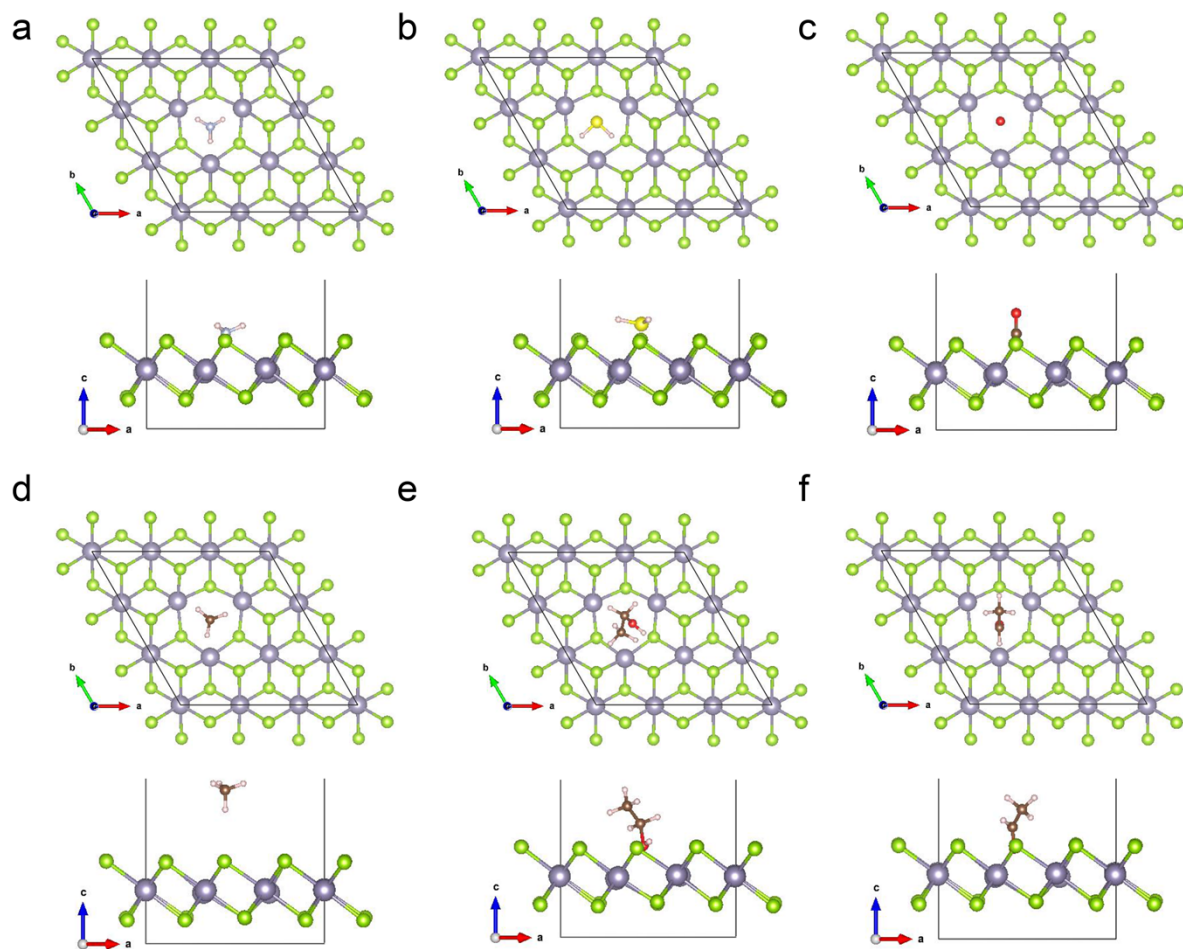


Figure S11. Optimized adsorption models on SnSe₂ with Se vacancies to (a) H₂S, (b) NH₃, (c) CO, (d) CH₄, (e) CH₃CH₂OH, and (f) CH₃CHO.

Table S2. Calculated adsorption parameters from different gas molecules to SnSe₂ monolayer with Se vacancies system.

SnSe ₂ system	Gas molecules	E _{ad} (eV)	d (Å)	h (Å)	ΔQ _b (e)
	SO ₂	-0.362	3.122	1.435	-0.149
	NH ₃	-0.703	3.035	-0.392	0.008
	H ₂ S	-0.576	3.100	0.907	0.019
SnSe ₂ with V _{Se}	CO	-0.344	3.376	0.540	-0.050
	CH ₄	-0.063	4.847	2.890	-0.002
	CH ₃ CH ₂ OH	-0.939	2.695	0.066	-0.009
	CH ₃ CHO	-1.031	2.620	-0.225	-0.018